

# QUADERNI di GEOFISICA

Low cost Structure-from-Motion-based  
fast surveying of a rock cliff:  
precision and reliability assessment



ISTITUTO NAZIONALE DI GEOFISICA E VULCANOLOGIA

156

**Direttore Responsabile**

Valeria DE PAOLA

**Editorial Board**

Luigi CUCCI - Editor in Chief (luigi.cucci@ingv.it)  
Raffaele AZZARO (raffaele.azzaro@ingv.it)  
Christian BIGNAMI (christian.bignami@ingv.it)  
Mario CASTELLANO (mario.castellano@ingv.it)  
Viviana CASTELLI (viviana.castelli@ingv.it)  
Rosa Anna CORSARO (rosanna.corsaro@ingv.it)  
Domenico DI MAURO (domenico.dimauro@ingv.it)  
Mauro DI VITO (mauro.divito@ingv.it)  
Marcello LIOTTA (marcello.liotta@ingv.it)  
Mario MATTIA (mario.mattia@ingv.it)  
Milena MORETTI (milena.moretti@ingv.it)  
Nicola PAGLIUCA (nicola.pagliuca@ingv.it)  
Umberto SCIACCA (umberto.sciacca@ingv.it)  
Alessandro SETTIMI (alessandro.settimi1@istruzione.it)  
Andrea TERTULLIANI (andrea.tertulliani@ingv.it)

**Segreteria di Redazione**

Francesca DI STEFANO - Coordinatore  
Rossella CELI  
Barbara ANGIONI

redazionecen@ingv.it

**REGISTRAZIONE AL TRIBUNALE DI ROMA N.174 | 2014, 23 LUGLIO**

© 2014 INGV Istituto Nazionale di Geofisica e Vulcanologia  
Rappresentante legale: Carlo DOGLIONI  
Sede: Via di Vigna Murata, 605 | Roma



ISTITUTO NAZIONALE DI GEOFISICA E VULCANOLOGIA

# QUADERNI di GEOFISICA

## Low cost Structure-from-Motion-based fast surveying of a rock cliff: precision and reliability assessment

Arianna Pesci<sup>1</sup>, Giordano Teza<sup>2</sup>, Fabiana Loddo<sup>1</sup>

<sup>1</sup>INGV | Istituto Nazionale di Geofisica e Vulcanologia, Sezione di Bologna

<sup>2</sup>Università degli Studi di Padova | Dipartimento di Geoscienze

Accepted 25<sup>th</sup> June 2019 | *Accettato 25 giugno 2019*

How to cite | *Come citare* Pesci A. et al., (2019). Low cost Structure-from-Motion-based fast surveying of a rock cliff: precision and reliability assessment. *Quad. Geofis.*, 156: 1-22.

Cover | *Comparison between TLS and SfM scaled using polylines point clouds* | *In copertina Un confronto tra la nuvola di punti TLS e quella SfM scalata col metodo della polilinea*

156



# INDEX

<b>Abstract</b>	<b>7</b>
<b>Introduction</b>	<b>7</b>
<b>1. Surveys and data processing</b>	<b>8</b>
<b>2. Comparison between the models</b>	<b>12</b>
<b>3. Discussion</b>	<b>13</b>
<b>4. Conclusions and future works</b>	<b>16</b>
<b>References</b>	<b>17</b>



# Abstract

Structure-from-Motion (SfM) performance was studied in terms of point clouds repeatability from a fast, low cost survey of an inaccessible slope carried out by means of a prosumer camera in emergency conditions and without ground control points. A rock cliff was observed from a distance of  $\sim 340$  m and the resulting point clouds were scaled with each other with the method of homologous polylines. A terrestrial laser scanning survey was carried out in order to scale the SfM data and evaluate the results. Tests of repeatability showed standard deviations (SDs) of 11 mm and 18 mm for point clouds obtained from images taken with focal lengths of 98 mm and 55 mm respectively. In order to evaluate the performance in cases where no reference models are available, data scaling was repeated by using Google Earth data, obtaining SDs  $\sim 8-9$  % larger. Moreover, three times the SD turned out to be  $\sim 2.5$  times the ground sample distance, leading to a suggestion for a completely independent scaling if no other sources for metric correction are available.

---

## Introduction

Structure from Motion (SfM) is a survey technique that takes advantage of the developments of digital photogrammetry and computer vision. As in traditional digital photogrammetry, SfM provides a point cloud starting from a set of overlapped images acquired from multiple viewpoints [see, e.g. Luhmann et al., 2014]. Before the photogrammetric modeling, very efficient image algorithms for image registration allow a fully automatic or at least a quasi-completely automatic alignment of the input images. Thanks to the easy implementation of the data acquisition and processing, SfM is largely used in geological/geomorphological surveys [see e.g. Brunier et al., 2016].

As a SfM survey is carried out, a reasonable number of Ground Control Points (GCPs) evenly distributed in the scenario are measured by means of a GNSS network and/or a total topographical station. The GCP coordinates are then used to provide a metric point cloud defined in a suitable reference frame. Moreover, some SfM software packages allow the incorporation of these coordinates into the Bundle Adjustment (BA) procedure [Yan et al., 2017]. It is the case, e.g., of Photoscan [Agisoft, 2019]. The use of precise GCP coordinates in BA modeling leads to very good results in surveying of both natural surfaces [see e.g. Barrand et al., 2009] and building façades [Caroti et al., 2015]. In particular, SfM can profitably be used for unstable rock-slope assessment under the conditions that a sufficient number of images with adequate overlap are acquired and the reconstruction is tied to a good GCP network [O'Banion et al., 2018]. The dependence of the model reliability and precision from the distribution and precision of GCPs was investigated from several authors. In particular, Tonkin and Midgley [2016] and Al Halbouni et al., [2017] demonstrated the importance of a uniform GCP spatial distribution in those cases in which highly accurate products are required and also highlighted that the time-intensive nature of GCP collection requires a balance between GCP quantity and survey quality. The fact that a reliable GCP network based on differential GPS receivers, total topographical station or a combination of them requires devices whose cost is in the range 10,000-20,000 \$, or more, should be noted.

In some cases reliable GCPs cannot be used. For example, a survey could be carried out in emergency conditions where no time for the GCP measurement is available. The access to a potentially dangerous rock cliff could be very difficult or impossible. Or, simply, a team may not have adequate financial resources for the use of GCPs. If no GCP data are available, the SfM modeling leads to a non-metric point cloud whose use for the detection of possible

morphological changes requires a scaling by an appropriate scale factor (SF). This is because metric multitemporal 3D models defined in the same reference frame are required in order to evaluate possible surface variations, deformation patterns, volume involved in mass movements and other physical quantities. If a survey is carried out by means of an Aerial Unmanned System (UAS), the consumer-level positioning equipment of the UAS can be used to provide reliable topography products even if they have no survey-grade quality because the error is  $\sim 0.1\%$  of the flying height [Carbonneau and Dietrich, 2017].

If no accurate camera positions are available, a suitable procedure is necessary to find the required SF, for example the polyline method [Pesci et al., 2016].

Regardless to the specific platform (terrestrial, aerial or a combination of them), a SfM survey should provide a model whose precision and resolution are adequate for the specific application. The Ground Sampling Distance (GSD), i.e. the distance between the centers of two adjacent pixels measured on the observed surface, the amount of required images and the other main observation parameters, in particular camera position and orientation, acquisition distance, focal distance (if it can be selected), should be defined accordingly [Cali and Ambu, 2018].

The issues related to a very fast SfM survey of a rock cliff, carried out from a mean distance of  $\sim 340$  m and without GCPs, are studied and faced here, emphasizing on the reliability and precision of the obtained results, time necessary for data acquisition and processing, low cost and independence from other measurement techniques. In particular, the research aim was an evaluation of the repeatability of photogrammetric modeling in case of quick surveys of natural surfaces carried out in emergency conditions. For this reason, a vertical cliff having a relatively regular, quasi-planar shape and that can be easily observed from points at a quasi-constant distance was chosen. This cliff, which belongs to the Appennino Bolognese area (Italy), was observed in a very short temporal window of about one hour by using a prosumer camera two times for each considered focal length (55 mm and 98 mm), taking about 30 images for each survey, leading to four point clouds. A Terrestrial Laser Scanning (TLS) measurement was also carried out in order to provide a reference point cloud for data validation. Issues related to the use of geographic information, in particular data taken from the Google Earth (GE) imagery, are also evaluated.

## 1. Surveys and data processing

The chosen test area is a rock cliff within the “Riserva Naturale Contrafforte Pliocenico” (Bologna Province, Northern Italy). The area of Contrafforte Pliocenico (or Pliocene Mountain Spur) [Ricci Lucchi et al., 1981; Ente Parchi, 2019] consists of a 15 km long complex formed by rocky outcrops of Pliocene sandstone. It is transversal to the valleys of Setta, Savena, Zena, and Idice and is extended from Sasso Marconi to Monte delle Formiche. The rocks of this mountain spur come from the sedimentation of sands and gravels carried by Apennine torrents within a wide marine gulf in the Pliocene (5-2 Ma ago) which corresponds to large part of the current Appennino Bolognese. The fact that the Pliocene Mountain Spur was declared “Site of Community Importance and Special Protection Area” should be noted. The selected cliff is subvertical and  $\sim 100$  m high. The area of interest is the upper part of the wall, including the crown area (Figure 1). The SfM surveys were carried out by using a Nikon D3300 camera, which is a typical prosumer camera characterized by a good balance between performance and cost, having a 6000 x 4000 pixels sensor, 3.9  $\mu\text{m}$  pixel side and equipped with lens whose focal length,  $f$ , is in the range of 55-300 mm. Each survey was carried out by walking parallel to the rock wall for  $\sim 150$  m, along a road whose mean distance from the cliff was  $\sim 340$  m and from which the view was not obstructed (Figure 1). For each survey, 30-35 images were acquired. According to the good practice in photogrammetry [Micheletti et al., 2015], the images were highly



overlapped and each point of the rock cliff was taken several times from different viewpoints. In particular, the overlap varied from  $\sim 100\%$  (about the same area acquired from two different points) to no less than  $\sim 80\%$ . It is important to point out that all the images of a single survey were taken with a well-defined  $f$  ( $f = 55 \text{ mm}$  and  $f = 98 \text{ mm}$  in the described tests), subsequently used in the photogrammetric modeling carried out by means of PhotoScan. Since each survey at a defined  $f$  was repeated in order to carry out a repeatability test, four photogrammetric surveys were carried out.

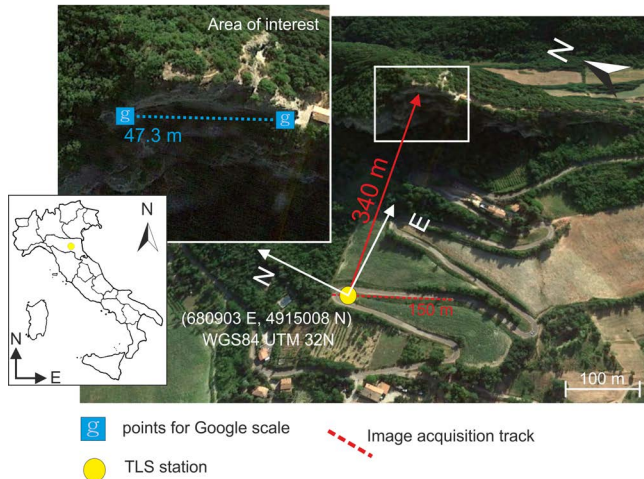


**Figure 1** Test area. The white square highlights the upper part of the rock wall, i.e. the area of interest. The red arrow is the distance between TLS and the area. The walk line along the road for image acquisition (dotted line) and the TLS position are also shown. Finally, the blue squares in the area of interest are two reference points that can be also recognized in GE imagery (background aerial image: © 2019 Google).

A baseline length was also defined on the basis of GE data by choosing two points (e.g. existing natural or artificial corners, blocks, topographical features) also visible in SfM images. In this way, the effect of use of available geographic information in emergency conditions can be evaluated, and, if necessary, adequately criticized.

In order to have reference data, a TLS-based survey was also carried out by means of an Optech ILRIS-3D ER instrument placed in front to the rock cliff at 245 m distance from its base; the mean acquisition distance was 340 m instead. A dense point cloud with a mean sampling step of  $\sim 3 \text{ cm}$  and  $\sim 10^6$  points was obtained.

Figure 2 shows the TLS-based point cloud of the area of interest, i.e. the upper part of the rock cliff, as well as the whole point cloud. The area of interest, which is  $\sim 80 \text{ m}$  width and  $40 \text{ m}$  high, is subvertical and has a cap shape. It should be noted that a feature can be recognized in a TLS-based point cloud by means of the intensity in near infrared band (1535 nm for the ILRIS-3D) and/or the geometric information. Two pairs of points were selected in the point clouds in order to provide an approximate scale factor to make metric the SfM point clouds (red circle points) and to measure the difference between a baseline measured from the TLS point cloud and the same extracted from GE (blue square points).

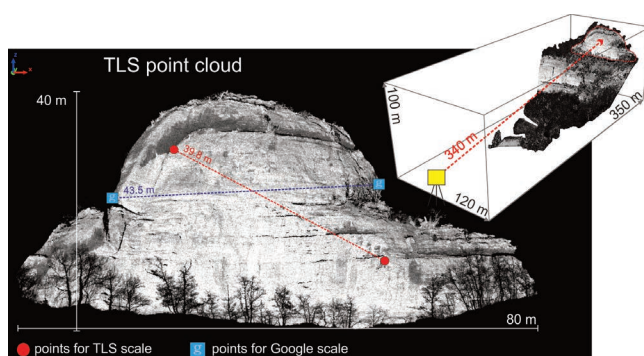


**Figure 2** TLS point cloud with intensity data. Red circles and blue squares will be used for scaling purposes.

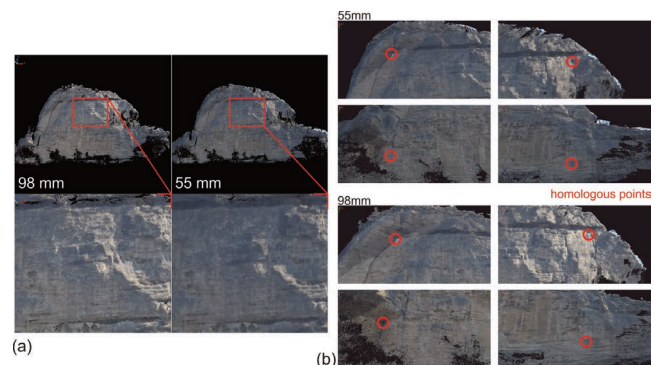
The SfM data processing led to four point clouds, each of which having  $\sim 107$  elements. They were called  $SfM_{1,55}$ ,  $SfM_{2,55}$ ,  $SfM_{1,98}$ ,  $SfM_{2,98}$ , where  $SfM_{i,f}$  indicates the  $i$ -th point cloud obtained by processing the images with focal length  $f$ . Since neither GCP nor camera coordinates were available, an appropriate method aimed at obtaining the SF was required. In this case, the method based on the comparison of length of polylines was used [Pesci et al., 2016]. Subsequently the SF-corrected point clouds were registered into a common reference frame.

In particular, the detailed procedure consisted of the following steps:

- (1) choice of a reference SfM point cloud. If point clouds characterized by different resolution are available, the reference should be chosen among those having the better resolution (in this case,  $SfM_{1,98}$  was chosen);
- (2) recognition in all the SfM point clouds of some homologous points which are well visible and widely distributed over the whole area. At least four points should be chosen. In order to allow a statistical analysis of the results and a subsequent reduction of the uncertainty, this recognition was carried out ten times for each point cloud;
- (3) creation, in each point cloud, of the closed polyline that connects the previously recognized points. According to the previous item, each polyline should be a trapezoid or, anyway, have at least four sides and be as large as possible in order to reduce the error propagation in the whole area. Moreover, the experiments suggest that the side lengths should have the same order of magnitude. Therefore, triangular polylines or oblong-shaped trapezoids should be avoided;
- (4) for each point cloud, computation of the ratios between the mean polyline length and the reference length (i.e. the mean of the polyline lengths belonging to the reference point cloud);
- (5) scaling of each point cloud on the basis of the previously defined ratio;
- (6) alignment of all the point clouds in a same reference frame by applying a rigid body transformation by means of a surface matching approach;
- (7) final scale correction aimed at obtaining metric point clouds.

Figure 3 shows two SfM point clouds and the recognized homologous points. It should be noted that the  $SfM_{1,98}$  point cloud is quite more detailed than the  $SfM_{1,55}$  one, as expected because of the different lens setting.

**Figure 3** (a) Two SfM point clouds obtained by processing of images taken with 55 mm and 98 mm focal length lens; (b) homologous points recognized in all the point clouds.



As outlined above, steps (2) and (3), the polylines were extracted 10 times for each point cloud in order to reduce the effect of the errors in recognition and selection of homologous points (Figure 4). Table 1 lists the obtained mean values ( $P_{n,f}$ ) together with the corresponding standard deviations and SFs with respect to the reference point cloud, i.e.  $SfM_{1,98}$ . The two last rows of Table 1 show values that are quite important here:  $T_{1,98}$  is the baseline length measured on

$SfM_{1_{98}}$  that corresponds to the baseline defined on the TLS point cloud, and  $G_{1_{98}}$  is the baseline length measured on  $SfM_{1_{98}}$  that corresponds to the GE baseline (Figs. 1 and 2).

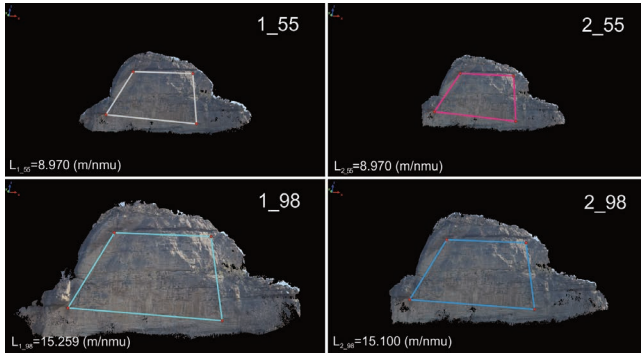


Figure 4 Polylines from the four SfM point clouds.

In order to obtain metric point clouds,  $SfM_{1_{98}}$  must be referred to a metric point cloud or at least a metric geographic dataset. Table 2 shows the baseline lengths and the corresponding partial scale factors. In particular,  $T_{TLS}$  is the baseline recognized in the TLS point cloud, which corresponds to  $T_{1_{98}}$ ;  $G_{GE}$  is the baseline recognized in the GE image, which corresponds to  $G_{1_{98}}$ ; and  $G_{TLS}$  is the baseline in the TLS point cloud that corresponds to the baseline recognized in the GE image ( $G_{GE}$ ). It should be noted that the  $G_{GE}$  length is 8% higher than the  $G_{TLS}$  one. Moreover, the standard deviation of  $G_{GE}$  is very high (1.7 m). These results are mainly due to two facts. First, the GE imagery is characterized by significant uncertainties, typically in the range 2-10% for a 50 m baseline [see e.g. Paredes-Hernandez et al., 2013; Goudarzi and Landry, 2017; Pulighe et al., 2017]. Second, a particular feature could not be easy to detect if seen from above. This means that, in the case of GE images, it would be more appropriate to talk about homologous areas instead of homologous points, i.e. a point in the same area could be selected instead of a same feature. This leads to another error source because both point detection and GE model errors contributes to make the reference lengths different. In addition, in an emergency survey there might be no time to check which points are visible in the GE images. More information about the precision of GE imagery is shown in Discussion. The fact that the standard deviation of GE baseline length recognized in the TLS point cloud ( $G_{TLS}$ ) is significantly higher than the polyline length recognized in the same point cloud ( $T_{TLS}$ ), i.e. 0.44 m vs. 0.06 m, should also be noted (Table 2). The ratio between the metric lengths from TLS and GE provides two further scale factors: the first one to scale SfM point clouds in the metric TLS reference frame, and the second one to scale SfM point clouds in the GE reference frame. Finally, the complete SFs for the conversion into metric point clouds are summarized in Table 3.

Polyline	$L$ (nmu)	$\sigma_L$ (nmu)	$SF_{1_{98}}$ (m/nmu)
$P_{1_{55}}$	8.970	0.002	1.701
$P_{2_{55}}$	8.040	0.001	1.898
<b><math>P_{1_{98}}</math></b>	<b>15.259</b>	<b>0.001</b>	<b>1</b>
$P_{2_{98}}$	15.100	0.002	1.011
$T_{1_{98}}$	4.570	0.001	-
$G_{1_{98}}$	5.131	0.002	-

Table 1 Length of polylines,  $L$ , corresponding standard deviation,  $\sigma_L$ , and scale factors computed with respect to the reference point cloud  $SfM_{1_{98}}$  (row highlighted by means of bold font), where nmu means “non metric unit”.

**Table 2** Lengths from TLS point cloud and GE data. The partial metric scale factors SFPM are to be multiplied to the ones in Table 1.

Baseline	$L$ (m)	$\sigma_L$ (m)	$SF_{PM}$ (m/nmu)
$T_{TLS} (T_{1,98})$	39.788	0.006	8.71
$G_{GE} (G_{1,98})$	47.320	1.7	8.49
$G_{TLS} (G_{GE})$	43.550	0.44	-

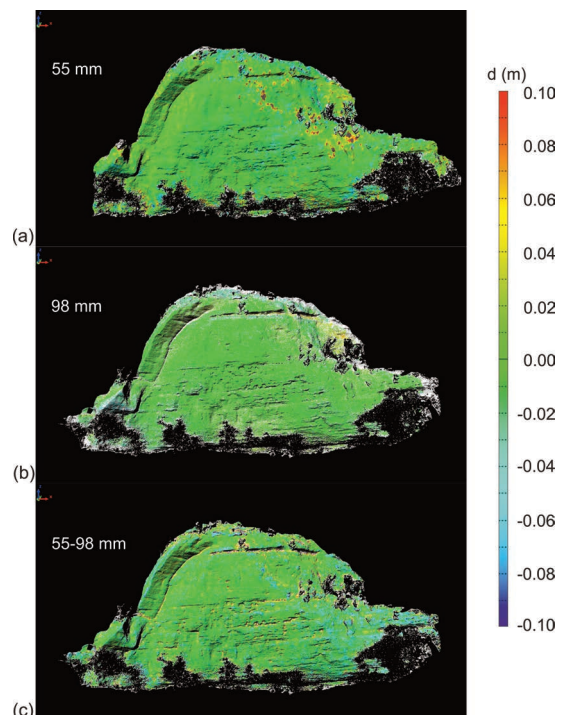
**Table 3** Final scale factor to obtain metric SfM point clouds by means of a reference length from TLS and GE.

SfM	$SF_{TLS}$ (m/nmu)	$SF_{GE}$ (m/nmu)
$P_{1,55}$	14.81	14.44
$P_{2,55}$	16.52	16.11
<b><math>P_{1,98}</math></b>	<b>8.71</b>	<b>8.49</b>
$P_{2,98}$	8.80	8.58

## 2. Comparison between the models

In order to evaluate the repeatability of SfM modeling, the metric SfM point clouds were aligned and compared leading to the difference maps. This task was carried out by means of the PolyWorks software package [Innovmetric, 2018]. Figure 5 shows the differences maps between the pair of point clouds generated from  $f = 55$  mm images (Figure 5a), between the pair of point clouds generated from  $f = 98$  mm images (Figure 5b) and, finally, between a  $f = 55$  mm and a  $f = 98$  mm SfM point cloud. The results of the statistical analysis, in terms of means of differences  $d$  and the corresponding standard deviations  $\sigma_d$ , are summarized in Table 4. The distributions of differences are zero-centered with  $\sigma_d$  ranging from 18 to 11 mm, depending on  $f$ . The same approach was applied to point clouds scaled on the basis of GE data. Also in this case the distributions are zero-centered, but the  $\sigma_d$  values are  $\sim 8-9\%$  larger, as expected.

**Figure 5** Maps of differences,  $d$ , between SfM point clouds. (a) pair for  $f = 55$  mm ( $SfM_{1,55}, SfM_{2,55}$ ); (b) pair for  $f = 98$  mm ( $SfM_{1,98}, SfM_{2,98}$ ); (c) comparison between  $SfM_{1,55}$  and  $SfM_{1,98}, SfM_{2,98}$ .



Compared point clouds	TLS-scaled		GE-scaled		%
	$d$ (m)	$\sigma_d$ (m)	$d$ (m)	$\sigma_d$ (m)	
$SfM_{1.55}, SfM_{2.55}$	0.000	0.018	0.000	0.020	8.2
$SfM_{1.98}, SfM_{2.98}$	0.000	0.011	0.000	0.012	8.3
$SfM_{1.98}, SfM_{1.55}$	0.000	0.014	0.000	0.015	8.5

**Table 4** Differences between aligned point clouds scaled by means of TLS data.

Other two comparisons were carried out between the TLS point cloud and the two metric point clouds obtained by scaling  $SfM_{1.98}$  with  $SF_{TLS}$  and  $SF_{GE}$ . As expected, in the first case the data were quite similar and the distribution of differences was characterized by a standard deviation of  $\sim 2$  cm, which corresponds to the TLS sampling step at the reference distance of  $\sim 340$  m (Figure 6a). In the second case, higher differences were found, with standard deviation of  $\sim 15$  cm (Figure 6b). Also this result was expected because of the worst precision of GE imagery. See below for a discussion of these aspects.

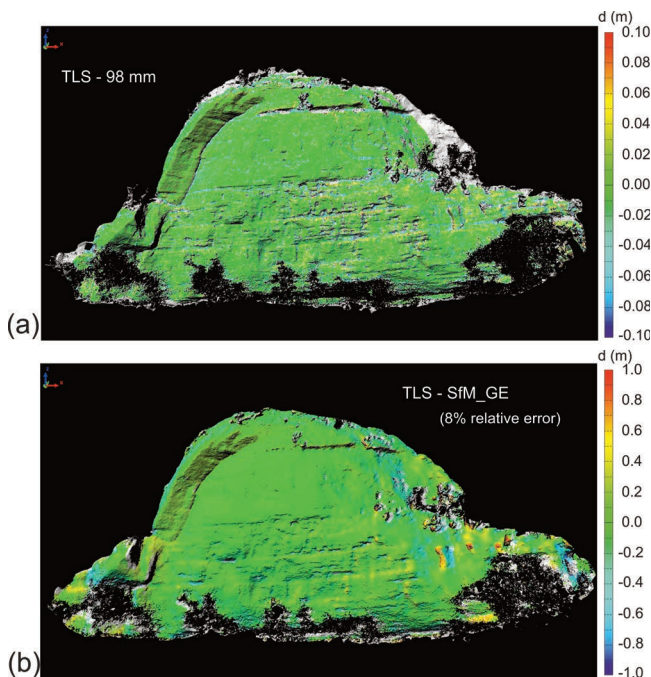


**Figure 6** Differences  $d$  between TLS and SfM point clouds ( $\cdot$ ): (a)  $SfM_{1.98}$  scaled by means of TLS data; (b)  $SfM_{1.55}$  scaled by means of GE data.

### 3. Discussion

Two pairs of image sets were taken for each of the two focal lengths  $f = 55$  mm and  $f = 98$  mm in order to evaluate the repeatability of SfM photogrammetric modeling in the case of terrestrial, long range (on average 340 m), independent and low cost surveys without GCPs. The SfM-based point clouds were scaled and therefore made metric by using two very different approaches: in the first case a baseline on a reference TLS point cloud was measured, leading to  $SF_{TLS}$ , and in the second one a baseline was taken and measured from GE imagery, leading to  $SF_{GE}$ . In the first case, a dense point cloud of the area of interest, or of at least a portion of this area, is required. In the second case,  $SF_{GE}$  is easily obtained from the freely available GE data, but the price to pay is the worse level of precision.

The GE images are not orthorectified and, on the basis of the area (major city or at least very

important area, small town, rural area), their source (satellite or aerial platform), resolution and positional precision are very different. The precision of GE imagery was investigated by several authors. For example, Pulighe et al., [2017] studied the horizontal accuracy of very high resolution GE images in the city of Rome (Italy), finding an overall positional accuracy, in terms of Root Means Square Error (RMSE), close to 0.7-1 m, sufficient for deriving ground truth samples, measurements, as well as large-scale planimetric maps. Goudarzi and Landry, [2017] found similar results in Montreal (Canada) and, moreover, highlighted that the misfit ranges from 0.13 to 2.7 m depending on the specific place and with a trend in southwest-northeast direction. In rural areas the RMSE can reach 5 m [Paredes-Hernandez et al., 2013]. In case of satellite images, the specific satellite and imager could be identified and the corresponding precision and resolution could therefore be checked. Moreover, it should be noted that there are effects related to the different point of view. Terrestrial photogrammetric surveys are described here, whereas GE images come from satellite or airplane/helicopter/drone. A quasi-horizontal baseline should therefore be considered, but also in this case there are effects related to uncertainty in vertical positioning (an error of about  $10^\circ$  in angular positioning of a 50 m long baseline leads to a length error near to 1 m). All these facts imply that, for a 50 m baseline, the error on its length can be in the range 2-10%, and the value is not known in advance. In particular, the error could reach ~2% in an urban area only, whereas is 8-10% in a mountain area. Therefore, until proven otherwise, a prudential 10% uncertainty should be taken into account for GE data.

As summarized in Table 4, the statistical distribution of differences in the two cases of TLS- based and GE-based scaling are quite similar, but the errors from GE-scaled point clouds are ~8% greater. As regards the magnitude of differences, what was achieved is similar to the literature results. The use of GE data for scaling does not affect the model shape because a same similarity transformation is applied to the whole point cloud.

The results show that a simple GE-based data scaling can be used at least in emergency conditions or where no alternatives are yet available. Nevertheless, the quality of GE data is not always known in advance, and could be significantly different in neighboring areas. This fact should be adequately taken into account.

GE images were used here. Nevertheless, data from other databases could be used. For example, digital orthoimages having 30 cm resolution obtained from data provided by WorldView-3 satellite are available [Vajsova et al., 2015]. Similarly, Pléiades 1A/1B form a very high resolution satellite constellation that allow the generation of 50 cm orthoimages [Agrafiotis and Georgopoulos, 2015]. In these cases, orthorectified data having well defined accuracy and resolution are available, but the related products should be purchased. Anyway, use of orthorectified images can allow a better recognition of homologous points because accurate elevation data are embedded in a GeoTIFF file. In conclusion, better results can be obtained because not only the data quality is higher and well known, but also because the choice of extreme points of a reference line in an orthoimage can be made in a better way.

If a completely independent survey of an area is necessary, because fast measurements must be carried out under emergency conditions on an inaccessible rock cliff, or also because no adequate financial resources are available, the GE imagery can therefore be used to have a first, rough modeling. Each survey was carried out in about half an hour (excluding traveling time). The data were processed by using a typical currently available workstation (Intel® Core® i7 CPU, 2.40 GHz clock, 16 Gb RAM). Once the method was defined, the photogrammetric modeling was carried out by means of PhotoScan out in about four hours and the data scaling, registration and analysis were carried out in about two hours. This means that the preliminary results based on GE-scaled (or, if available, TLS-based) data can be obtained in a working day and, therefore, are fully compatible with the needs of a survey in emergency conditions. A fast, rough evaluation of possible changes, e.g. mass loss because of rockfall or displacements due to an incipient toppling is therefore possible. If the discrepancy is ~10%, the internal precision

of SfM terrestrial point clouds is assured, even if a critical approach is required at the stage of interpretation of the results. Nevertheless, if very accurate metric point clouds are required, a correction of the results is necessary. Moreover, the use of GCPs is required whenever possible [Micheletti et al., 2015; Brunier et al., 2016].

Since the point cloud scaling is initially carried out with respect to a SfM-based point cloud by means of the polyline method, and in particular several polylines are extracted in order to minimize the relative scaling error, all the point clouds can be easily and quickly registered into a same reference frame. Therefore, the final scaling aimed at obtaining metric point clouds, which may be based on GE data, does not act on morphology and relative positions, which are conditioned solely by the precision of photogrammetric modeling without GCPs. This means that, if multitemporal data are available, the methods aimed at computing the displacement field by means of piecewise surface matching [Teza et al., 2007] or correlation techniques [Travelletti et al., 2013] can be used. Clearly, the magnitude and precision of the final velocities depend on the final scaling.

$f$ (mm)	$3\sigma_{\text{TLS}}$ (m)	$3\sigma_{\text{GE}}$ (m)	GSD (m)	$3\sigma_{\text{TLS}}/\text{GSD}$	$3\sigma_{\text{GE}}/\text{GSD}$
55	0.054	0.059	0.025	2.3	2.5
98	0.033	0.036	0.011	2.9	3.2
			mean:	2.5	2.9

**Table 5** Ratio between  $3\sigma$  of point cloud differences and GSD size at 340 m reference distance.

It is interesting to correlate the results with the Ground Sample Distance (GSD) at a given reference distance, i.e. the distance between the centers of two adjacent pixels of an image on the observed surface. This quantity is  $GSD = pd / f$ , where  $p$  is the sensor pixel size and  $d$  is the acquisition distance. Table 5 summarizes the ratios between the  $3\sigma$  values of the difference distributions, which can be considered as the noise and therefore the minimum size of possible changes that could be detected, and the GSD. Values range from 2.3 to 2.9 (mean: 2.5) for TLS-scaled point clouds and from 2.5 to 3.2 (mean: 2.9) for GE-scaled ones. Also in this case the difference between TLS-based and GE-based data is  $\sim 8\%$ .

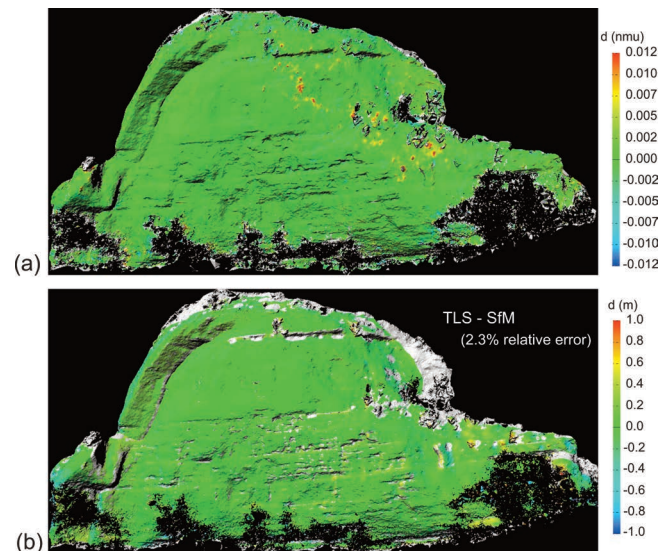
These results are like the ones obtained from Caroti et al. [2015], which found a RSME 2-4 times the GSD if 6-12 GCPs evenly distributed on a building façade are used to constrain the photogrammetric modelling, and a RSME 3-5 times the GSD if no GCPs are used. The importance of the GCP distribution depending on topography was highlighted by Al-Halbouni et al. [2017], which also demonstrated that too many GCPs do not provide better results.

The obtained results suggest a completely independent way to provide a first rough estimate of the SF without GE data. If the ratio  $3\sigma / \text{GSD}$  is 2.5 for a metric or at least a quite metric SfM point cloud, this value can be used for correcting the scale of a less metrically accurate SfM point cloud. In order to test this idea, a trial was done by using the  $SfM_{1,55}$  point cloud in its original form. Table 3 shows that the SF to transform the initial, non-metric coordinates into metric ones is  $SF_{\text{TLS}} = 14.81$  m/nmu. The standard deviation of the difference map between  $SfM_{1,55}$  and  $SfM_{2,55}$  (the second point cloud is scaled to the first one) is 0.0014 nmu. Assuming that  $3\sigma / \text{GSD} = 2.5$  for a metric point cloud, it is  $3\sigma_{\text{nmu}} SF^* / \text{GSD} = 2.5$ , where  $SF^*$  is a first estimate of the scale factor, and therefore,  $SF^* = 14.5$  m/nmu, which differs by  $\sim 2\%$  from  $SF_{\text{TLS}}$ . Results are shown in Figure 7. Clearly, such an approach is valid for the specific camera in the specific observation conditions. Therefore, this result should be treated with care. Further researches are required to generalize it, i.e. to generalize the found value 2.5.

Finally, the fact that the obtained results do not depend from the used platform should be noted. Even if the tests were carried out by means of terrestrial SfM, the results should apply also in

case of a UAS-based observation under these conditions: (1) at least a prosumer camera is used; (2) the flight height is at least roughly constant, to have a constant mean acquisition distance; (3) the shape of the surveyed surface is compatible with a photogrammetric modeling without GCPs. It should be noted that a consumer drone could be equipped with a low quality camera whose performance is inadequate (in this case,  $3\sigma / \text{GSD} \approx 2.5$  could be invalid). Moreover, if a relatively long landslide is observed, the propagation of alignment and modeling errors could lead to unacceptably rough estimates. Anyway, further studies are required for UAS-based measurements.

**Figure 7** Map of differences: (a) initial comparison in a non-metric reference system between point clouds obtained from  $f = 55$  mm images, where the standard deviation of differences is 0.0014 nm; (b) comparison between the scaled  $SfM_{1,55}$  point cloud and the TLS point cloud.



## 4. Conclusions and future works

The results obtained by means of images of a rock cliff taken from  $\sim 340$  m distance and with the focal lengths  $f = 55$  mm and  $f = 98$  mm show that terrestrial, long range, independent and low cost surveys without GCPs can provide SfM point clouds whose precision is enough for a first characterization of the possible changes, under the condition that these changes are at least 2.5 times the ground sample distance. The SfM-based point clouds were made metric by means of either a reference TLS point cloud or GE imagery. Also the GE-based scaling can provide useful data, even if the precision is worsened by a factor of  $\sim 8-9$  %. Also taking into account the fact that the quality of GE data is not always known in advance, and could be significantly different in neighboring areas, the result highlight that a simple GE-based data scaling can be used at least in emergency conditions or where no alternatives are yet available.

It is worth emphasizing that the research is aimed at understanding what can be done with a prosumer camera in emergency conditions or in conditions where resources are very limited. Clearly, the use of GCPs is recommended to obtain accurate georeferenced photogrammetric models.

Future works will focus on experiments with artificial targets and in situ surveys for an adequate characterization of SfM-based point clouds precision and resolution obtainable in emergency conditions with prosumer and professional cameras in both terrestrial and aerial surveys.



## References

- Agisoft (2019). "Photoscan web page". Accessed 25 October 2019. <http://www.agisoft.com>
- Agrafiotis P. and Georgopoulos A., (2015). *Comparative assessment of very high resolution satellite and aerial orthoimagery*. The International Archives of the Photogrammetry, Remote Sensing and Spatial Information Sciences, XL-3/W2. doi:10.5194/isprsarchives-XL-3-W2-1-2015.
- Al-Halbouni D., Holohan E., Saberi L., Alrshdan H., Sawarieh A., Closson D., Walter T.R. and Dahm T., (2017). *Sinkholes, subsidence and subsosion on the eastern shore of the Dead Sea as revealed by a close-range photogrammetric survey*. *Geomorphology*, 285, 305-324.
- Barrand N.E., Murray T., James T.D., Barr S.L. and Mills J.P., (2009). *Optimizing photogrammetric DEMs for glacier volume change assessment using laser-scanning derived ground-control points*. *Journal of Glaciology*, 55(189), 106-116.
- Brunier G., Fleury J., Anthony J.E., Pothin V., Vella C., Dussouillez P., Gardel A. and Michaud E., (2016). *Structure-from-Motion photogrammetry for high-resolution coastal and fluvial geomorphic surveys*. *Géomorphologie*, 22(2), 147-161.
- Calì M. and Ambu R., (2018). *Advanced 3D photogrammetric surface reconstruction of extensive objects by UAV camera image acquisition*. *Sensors*, 18(9), 2815. doi:10.3390/s18092815.
- Carbonneau P.E. and Dietrich J.T., (2017). *Cost-effective non-metric photogrammetry from consumer-grade sUAS: implications for direct georeferencing of structure from motion photogrammetry*. *Earth Surface Processes and Landforms*, 42(3), 473-486.
- Caroti G., Martínez-Espejo Zaragoza I. and Piemonte A., (2015). *Accuracy assessment in Structure from Motion 3d reconstruction from UAV-born images: the influence of the data processing methods*. The International Archives of the Photogrammetry, Remote Sensing and Spatial Information Sciences, XL-1/W4, 103-109.
- Ente Parchi, (2019). *Riserva Naturale Contrafforte Pliocenico web site, English version* <<http://www.parks.it/riserva.contrafforte.pliocenico/Eindex.php>> (May2, 2019).
- Goudarzi M.A. and Landry R.Jr., (2017). *Assessing horizontal positional accuracy of Google Earth imagery in the city of Montreal, Canada*. *Geodesy Cartography*, 43(2), 56-65.
- Innovmetric, (2018). *PolyWorks Inspector web page*. <<http://www.innovmetric.com/en/products/polyworks-inspector>> (December 28, 2018).
- Micheletti N., Chandler J.H. and Lane S.N., (2015). *Structure from Motion (SfM) photogrammetry*. In: *Geomorphological Techniques* (L.E. Clarke and J.M. Nield, eds.), Chapter 2, Sect. 2. British Society of Geomorphology, London. <[https://dspace.lboro.ac.uk/dspace-jspui/bitstream/2134/17493/3/2.2.2\\_sfm.pdf](https://dspace.lboro.ac.uk/dspace-jspui/bitstream/2134/17493/3/2.2.2_sfm.pdf)> (June 19 2019).
- O'Banion M.S., Olsen M.J., Rault C., Wartman J. and Cunningham K., (2018). *Suitability of structure from motion for rock-slope assessment*. *Photogrammetric Record*, 33, 217-242.
- Paredes-Hernandez C.U., Salinas-Castillo W.E., Guevara-Cortina F. and Martinez-Becerra X., (2013). *Horizontal positional accuracy of Google Earth's imagery over rural areas: a study case in Tamaulipas, Mexico*. *Bulletin of Geodetic Sciences*, 19(4), 588-601.
- Pesci A., Teza G., Bisson M., Muccini F., Stefanelli P., Anzidei M., Carluccio R., Nicolosi I., Galvani A., Sepe V. and Carmisciano C., (2016). *A fast method for monitoring the coast through independent photogrammetric measurements: application and case study*. *International Journal of Geomatics and Geosciences*, 4(4), 73-81.
- Pulighe G., Baiocchi V. and Lupia F., (2016). *Horizontal accuracy assessment of very high resolution Google Earth images in the city of Rome, Italy*. *International Journal of Digital Earth*, 9(4), 342-362.
- Ricci Lucchi F., Colella A., Ori G.G., Oglioni F. and Colalongo M.L., (1981). *Pliocene fan deltas of the Intra-Apenninic Basin, Bologna*. In: *Excursion Guidebook for IAS 2nd Regional Meeting* (F. Ricci Lucchi, ed.), pp. 89-138, Bologna.
- Teza G., Galgaro A., Zaltron N. and Genevois R., (2007). *Terrestrial laser scanner to detect landslide displacement fields: a new approach*. *International Journal of Remote Sensing*, 28(16), 3425-3446.

- Tonkin N.T. and Midgley G.N., (2016). *Ground-Control Networks for Image Based Surface Reconstruction: An Investigation of Optimum Survey Designs Using UAV Derived Imagery and Structure-from-Motion Photogrammetry*. *Remote Sensing*, 8, 786. doi: 10.3390/rs8090786.
- Travelletti J., Delacourt C., Malet J.P., Allemand P., Schmittbuhl J. and Toussaint R., (2013). *Performance of Image Correlation Techniques for Landslide Displacement Monitoring*. In: *Landslide Science and Practice - Volume 2: Early Warning, Instrumentation and Monitoring* (C. Margottini, P. Canuti, K. Sassa, eds.), pp. 217-226. Springer, Berlin Heidelberg.
- Vajsová B., Walczynska A., Aastrand P., Barisch S. and Hain S., (2015). *New sensors benchmark report on WorldView-3*. Publications Office of the European Union, EUR 27673 EN. doi:10.2788/237561.
- Yan L., Chen R., Sun H., Sun Y., Liu L. and Wang Q., (2017). *A novel bundle adjustment method with additional ground control point constraint*. *Remote Sensing Letters*, 8(1), 68-77, doi: 10.1080/2150704X.2016.1235809.



# QUADERNI di GEOFISICA

ISSN 1590-2595

<http://istituto.ingv.it/le-collane-editoriali-ingv/quaderni-di-geofisica.html/>

I QUADERNI DI GEOFISICA (QUAD. GEOFIS.) accolgono lavori, sia in italiano che in inglese, che diano particolare risalto alla pubblicazione di dati, misure, osservazioni e loro elaborazioni anche preliminari che necessitano di rapida diffusione nella comunità scientifica nazionale ed internazionale. Per questo scopo la pubblicazione on-line è particolarmente utile e fornisce accesso immediato a tutti i possibili utenti. Un Editorial Board multidisciplinare ed un accurato processo di peer-review garantiscono i requisiti di qualità per la pubblicazione dei contributi. I QUADERNI DI GEOFISICA sono presenti in "Emerging Sources Citation Index" di Clarivate Analytics, e in "Open Access Journals" di Scopus.

QUADERNI DI GEOFISICA (QUAD. GEOFIS.) welcome contributions, in Italian and/or in English, with special emphasis on preliminary elaborations of data, measures, and observations that need rapid and widespread diffusion in the scientific community. The on-line publication is particularly useful for this purpose, and a multidisciplinary Editorial Board with an accurate peer-review process provides the quality standard for the publication of the manuscripts. QUADERNI DI GEOFISICA are present in "Emerging Sources Citation Index" of Clarivate Analytics, and in "Open Access Journals" of Scopus.

# RAPPORTI TECNICI INGV

ISSN 2039-7941

<http://istituto.ingv.it/le-collane-editoriali-ingv/rapporti-tecnici-ingv.html/>

I RAPPORTI TECNICI INGV (RAPP. TEC. INGV) pubblicano contributi, sia in italiano che in inglese, di tipo tecnologico come manuali, software, applicazioni ed innovazioni di strumentazioni, tecniche di raccolta dati di rilevante interesse tecnico-scientifico. I RAPPORTI TECNICI INGV sono pubblicati esclusivamente on-line per garantire agli autori rapidità di diffusione e agli utenti accesso immediato ai dati pubblicati. Un Editorial Board multidisciplinare ed un accurato processo di peer-review garantiscono i requisiti di qualità per la pubblicazione dei contributi.

RAPPORTI TECNICI INGV (RAPP. TEC. INGV) publish technological contributions (in Italian and/or in English) such as manuals, software, applications and implementations of instruments, and techniques of data collection. RAPPORTI TECNICI INGV are published online to guarantee celerity of diffusion and a prompt access to published data. A multidisciplinary Editorial Board and an accurate peer-review process provide the quality standard for the publication of the contributions.

# MISCELLANEA INGV

ISSN 2039-6651

[http://istituto.ingv.it/le-collane-editoriali-ingv/miscellanea-ingv.html](http://istituto.ingv.it/le-collane-editoriali-ingv/miscellanea-ingv.html/)

MISCELLANEA INGV (MISC. INGV) favorisce la pubblicazione di contributi scientifici riguardanti le attività svolte dall'INGV. In particolare, MISCELLANEA INGV raccoglie reports di progetti scientifici, proceedings di convegni, manuali, monografie di rilevante interesse, raccolte di articoli, ecc. La pubblicazione è esclusivamente on-line, completamente gratuita e garantisce tempi rapidi e grande diffusione sul web. L'Editorial Board INGV, grazie al suo carattere multidisciplinare, assicura i requisiti di qualità per la pubblicazione dei contributi sottomessi.

MISCELLANEA INGV (MISC. INGV) favours the publication of scientific contributions regarding the main activities carried out at INGV. In particular, MISCELLANEA INGV gathers reports of scientific projects, proceedings of meetings, manuals, relevant monographs, collections of articles etc. The journal is published online to guarantee celerity of diffusion on the internet. A multidisciplinary Editorial Board and an accurate peer-review process provide the quality standard for the publication of the contributions.

**Coordinamento editoriale e impaginazione**

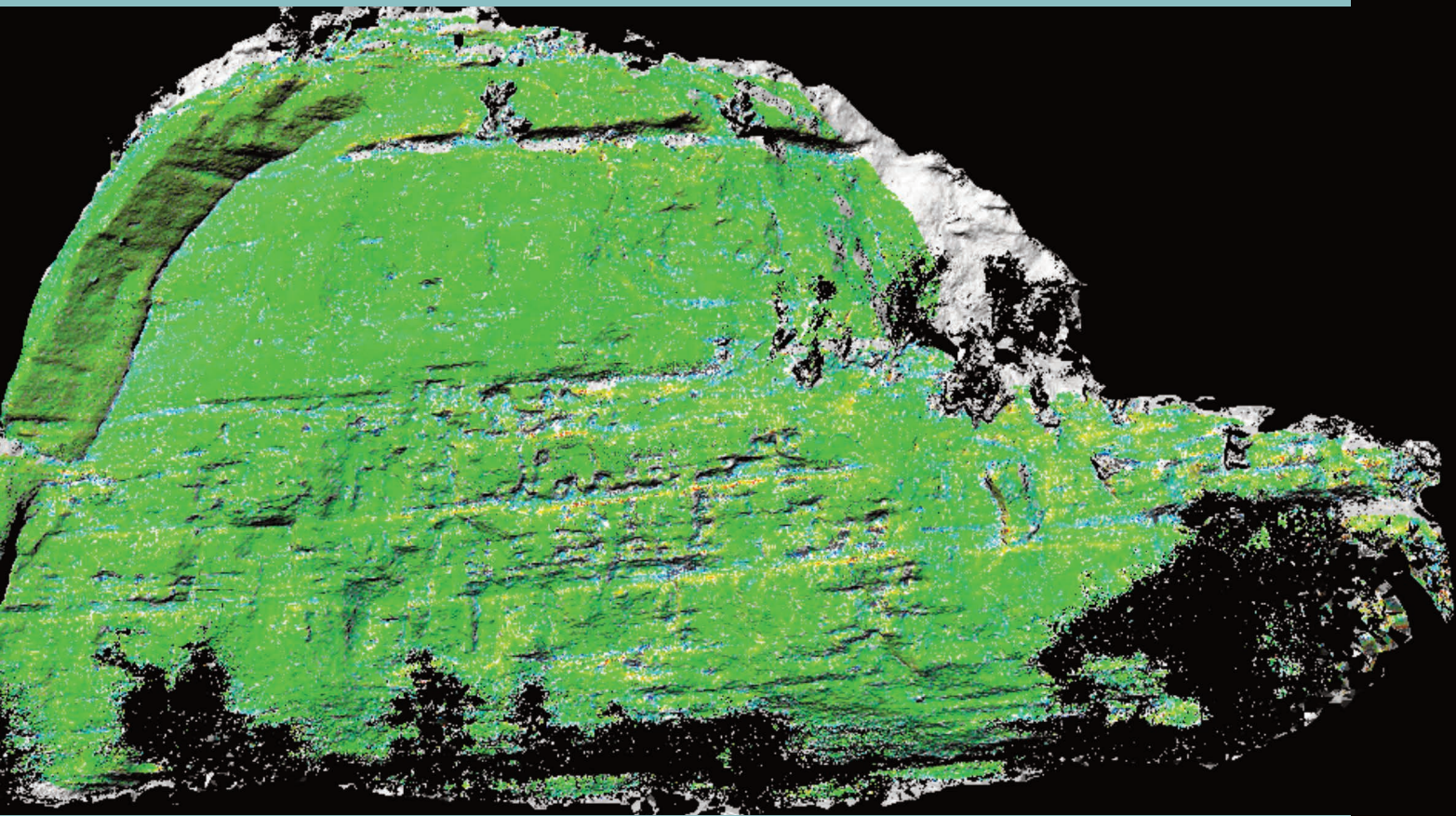
Francesca DI STEFANO, Rossella CELI  
Istituto Nazionale di Geofisica e Vulcanologia

**Progetto grafico e impaginazione**

Barbara ANGIONI  
Istituto Nazionale di Geofisica e Vulcanologia

©2019  
Istituto Nazionale di Geofisica e Vulcanologia  
Via di Vigna Murata, 605  
00143 Roma  
tel. +39 06518601

[www.ingv.it](http://www.ingv.it)



ISTITUTO NAZIONALE DI GEOFISICA E VULCANOLOGIA

